Fusion of electroencephalography and functional magnetic resonance imaging to explore epileptic network activity

Borbála Hunyadi*[†], Wim Van Paesschen[‡§], Maarten De Vos[¶] and Sabine Van Huffel*[†]

*Stadius Center for Dynamical Systems, Signal Processing and Data Analytics,
Department of Electrical Engineering (ESAT) KU Leuven, Belgium

[†]iMinds Medical IT, Belgium

[‡]Laboratory for Epilepsy Research, UZ Leuven & KU Leuven, Leuven, Belgium

[§]Medical Imaging Research Center, UZ Leuven & KU Leuven, Leuven, Belgium

[¶]Institute of Biomedical Engineering, Department of Engineering Science, Oxford University, Oxford, United Kingdom

Email: borbala.hunyadi@esat.kuleuven.be

Abstract—Electroencephalography (EEG) and functional magnetic resonance imaging (fMRI) are two complementary modalities capturing a mixture of various underlying neural sources. The fusion of these modalities promises the best of both worlds, i.e. a better resolution in time and space, respectively. Assuming that EEG and fMRI observations are generated by the same mixing system in both modalities, their fusion can be achieved by joint blind source separation (BSS). We solve the joint BSS problem using different variants of joint independent component analysis (jointICA) and coupled matrix-tensor factorization (CMTF). We demonstrate that EEG-fMRI fusion provides a detailed spatio-temporal characterization of an EEG-fMRI dataset recorded in epilepsy patients, leading to new insights in epileptic network behaviour.

I. INTRODUCTION

EEG and fMRI are two complementary modalities to record and study brain function. They are complementary not only in the sense that they record different aspects of brain activity - electrical activity and blood oxygen level, respectively - but also because of their reciprocal temporal and spatial resolution. Therefore, integrating EEG-fMRI information offers a better characterization of brain function and has proven useful in various applications including cognitive functioning, schizophrenia or epilepsy. Integration may be performed using different approaches, among which data fusion offers true interaction between the modalities, by assigning symmetrical roles and simultaneously processing them [1]. We fuse EEG and fMRI data based on the following assumptions. We consider various brain sources which are active during the recordings. Both modalities capture a linear mixture of the true underlying source activities. The mixing system is determined purely based on the relative strength of each source, therefore, it is the same for both modalities. In this case, the underlying sources can be retrieved using joint BSS of the EEG and fMRI data. Our goal is to investigate different approaches to solve the joint BSS problem.

One way to tackle this problem is to impose independence between the sources using jointICA [2], [3]. A drawback of this method is that it can only take into account a single EEG channel, losing information about the spatial diversity of multichannel EEG. An extension of jointICA has been proposed recently [4], that allows to take into account multichannel EEG information by spatial or temporal concatenation. Still, this approach can not exploit the inherent multidimensional structure of EEG, as concatenation destroys the spatial or temporal interdependence of the multichannel signals. Alternatively, the joint BSS problem can be formulated as a coupled matrix-tensor factorization (CMTF). This approach has two very important advantages. First, the tensor representation of EEG allows to fully exploit the higher order structure of EEG. Second, within CMTF, the tensor is factorized using canonical polyadic decomposition, which leads to very simple and mild uniqueness conditions.

The paper is structured as follows. First, we explain our signal model and the assumptions. Afterwards, we give the mathematical formulation of the joint BSS problem and its solutions using jointICA and CMTF approaches. Finally, we apply these techniques to fuse EEG-fMRI data recorded from epilepsy patients to achieve a detailed spatio-temporal characterization of interictal network activity.

II. METHODS

A. Signal model

We consider simultaneously recorded EEG and fMRI measurements in a group of patients under the same experimental conditions. We assume that the same neural processes are recruited during the experiment in all patients, and that these neural processes are reflected in both modalities. We further assume that each modality is preprocessed to eliminate the effect of artifacts, and analysed using well-established methods in the specific application domain in order to obtain relevant and reliable information about the neural processes of interest. In particular, we work with average EEG waveforms and fMRI activation maps. By activation map we mean a vector of voxel intensities, where the intensity in a given voxel reflects whether BOLD signal fluctuations are consistent with the occurrence of interictal spikes. As a result, the observed EEG signals and

fMRI activations are generated as a mixture of the underlying neural processes of interest. The mixing system reflects the level of neural involvement, i.e. how strongly each neural process is present in each patient. Formally, let $\mathbf{s}_i$ indicate the ith neural source. The activity of this particular source is observed as a certain waveform on the multichannel EEG, denoted by S_i^{EEG}, and an activation map in the fMRI, denoted by $\mathbf{s}_i^{fMRI}$. The EEG-fMRI observations can be organized in the rows of the source tensor $\mathcal{S}^{EEG} \in \mathbb{R}^{I \times J \times K}$ and source matrix $S^{fMRI} \in \mathbb{R}^{I \times L}$, where I is the number of neural sources, J is the number of EEG channels, K is the number of time samples and L is the number of fMRI voxels. Then, the EEG signals $\mathcal{X}^{EEG} \in \mathbb{R}^{M \times J \times K}$ and fMRI activations $X^{fMRI} \in \mathbb{R}^{M \times L}$ observed in all M participants can be written as

$$\mathcal{X}^{EEG} = \mathcal{S}^{EEG} \times_1 A$$
$$X^{fMRI} = S^{fMRI} \times_1 A = AS^{fMRI} \tag{1}$$

where $\times_1$ denotes the mode-1 tensor-matrix product. Analogously to the matrix product, A makes linear combinations of the columns of $\mathcal{S}^{EEG}$. The matrix $A \in \mathbb{R}^{M \times I}$ describes the mixing system. In particular, the entry $a_{m,i}$ reflects how strongly the ith neural source is involved in participant m.

Our goal is to solve the joint blind source separation problem in eq. (1), i.e. to retrieve the unknown mixing matrix A and the underlying sources $\mathcal{S}^{EEG}$ and S^{fMRI} only based on the observations $\mathcal{X}^{EEG}$ and X^{fMRI}. In the following sections we present different multimodal fusion techniques which we will apply to this end.

B. JointICA

JointICA [2] solves eq. (1) by taking into account a single EEG channel, where the pattern of interest is most prominent. The observed data of the two modalities are concatenated to form a joint observation matrix. Then, the problem is formulated as follows:

$$[X_{(j)}^{EEG} X^{fMRI}] = A[S_{(j)}^{EEG} S^{fMRI}] \tag{2}$$

Here, $X_{(j)}^{EEG}$ denotes the multisubject EEG pattern on the selected channel j. Accordingly, the source matrix $S_{(j)}^{EEG}$ reveals the source waveforms on channel j. JointICA solves the BSS problem by assuming that the joint sources $[s_{(j),i}^{EEG} s_i^{fMRI}]$ are statistically independent from each other. The relative strength of the sources across patients are reflected in the columns of the mixing matrix A, which is shared between the two modalities. Therefore, our original assumption that the strengths of the neural sources are reflected the same way in both modalities, are automatically kept.

C. Multichannel jointICA

Multichannel extensions of jointICA were proposed by Swinnen et al [4]. In t-jointICA the information from multiple channels are concatenated in time to form a long observation matrix. The joint BSS problem is now formulated as follows:
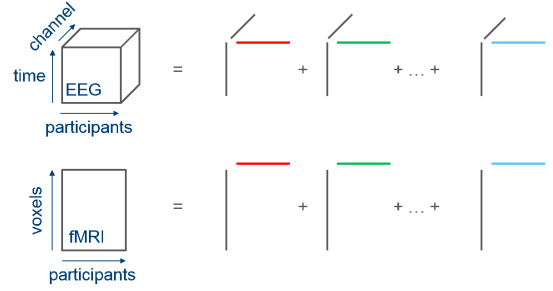

Fig. 1: Visual representation of the coupled matrix tensor factorization of the fMRI and EEG dataset, with shared signatures in the patient dimension.

$$[X_{(1)}^{EEG} \dots X_{(j)}^{EEG} \dots X_{(J)}^{EEG} X^{fMRI}] =$$
$$= A[S_{(1)}^{EEG} \dots S_{(j)}^{EEG} \dots S_{(J)}^{EEG} S^{fMRI}] \tag{3}$$

D. CMTF

The coupled matrix-tensor factorization (CMTF) solves the joint BSS problem in eq. (1) directly, without the need of selecting or reorganizing the slices of the tensor. As such, it allows to exploit the three-way structure of the tensor. A visual representation of this factorization is shown in Figure 1. CMTF is formulated as the minimization of the objective function in eq. (4):

$$f(A, P, Q, S^{fMRI}) =$$
$$= ||X^{fMRI} - AS^{fMRI}||^2 + ||\mathcal{X}^{EEG} - \sum_R \mathbf{a}_r \circ \mathbf{p}_r \circ \mathbf{q}_r||^2 \tag{4}$$

where $\mathbf{a}_r$, $\mathbf{p}_r$ and $\mathbf{q}_r$ denote the rth column of the matrices A, P and Q. Note that $\mathcal{X}^{EEG} = \sum_R \mathbf{a}_r \circ \mathbf{p}_r \circ \mathbf{q}_r$ is the canonical polyadic decomposition (CPD) of the tensor $\mathcal{X}^{EEG}$. CPD is unique under mild conditions, and the uniqueness of S^{fMRI} is also guaranteed in case A has full column rank [5]. As such, the unique sources can be retrieved without assuming independence or any other constraints on the sources. We implemented the minimization problem in eq. (4) using Tensorlab [6], [7].

E. Restricted CMTF

Although CPD and therefore CMTF is unique under mild conditions, prior knowledge may be incorporated into the decomposition in the form of constraints on the factors in order to facilitate robustness against noise and physical interpretation [11]. Recall our main assumption, that the EEG and fMRI observations are a mixture of underlying neural sources and that the mixing system is determined by the patient-by-patient variability of the strength of these processes. Based on certain EEG features we can estimate the patient-by-patient variability and fix the patient dimension signatures accordingly, leading to a restricted CMTF approach. More details on the motivation
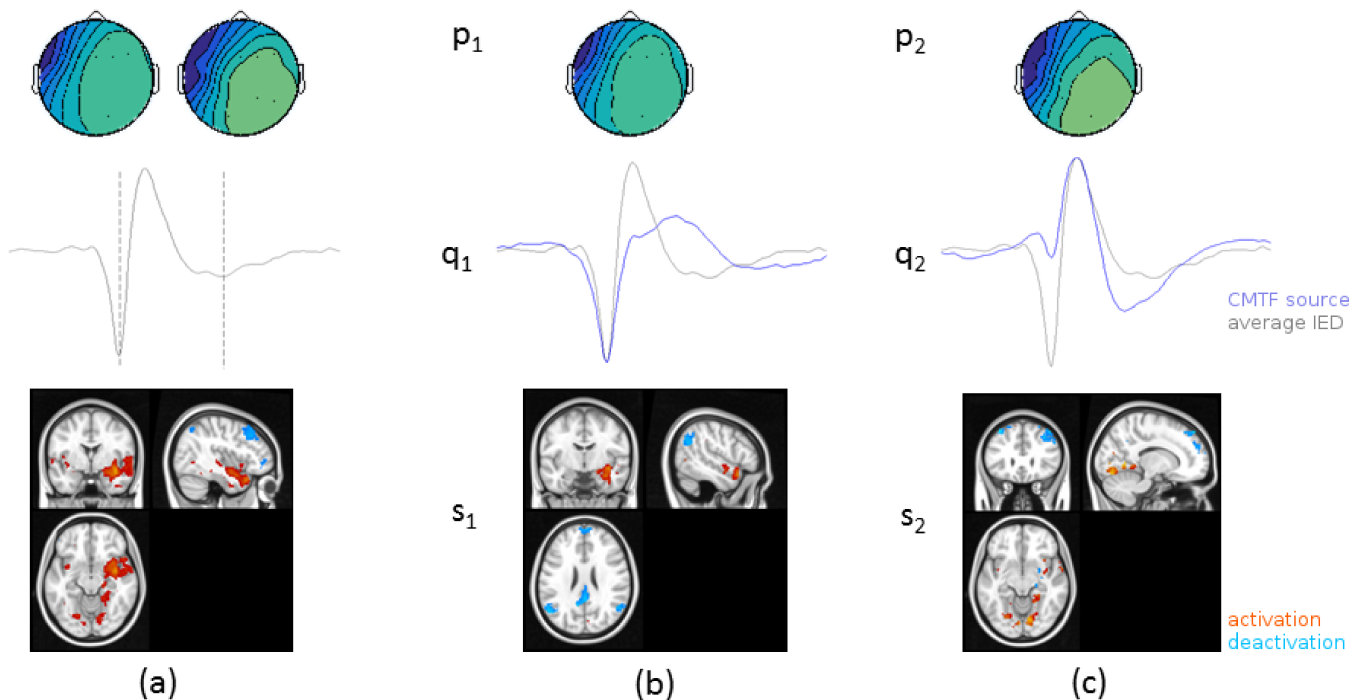
Fig. 2: Spatiotemporal characterization of the interictal epileptic network measured by EEG-fMRI. The multipatient average IED and activation map is shown in (a). Two components were extracted by restricted CMTF, their channel, temporal and voxel signatures are shown in (b) and (c).

behind this approach and the estimation of the patient-by-patient variability will be discussed in the results section after presenting the EEG and fMRI observations.

F. Experimental data

Simultaneous EEG and fMRI data of 5 right temporal and 5 left temporal lobe epilepsy patients were used in this study. Scalp EEG was recorded with an MR compatible EEG cap placed according to the international 10/20 system. The EEG was bandpass filtered between 0.1 and 30 Hz, gradient artifacts and ballistocardiographic artifacts were removed using the Bergen plug-in for EEGLAB and Brain Vision Analyzer software, respectively. Interictal epileptic discharges (IEDs) were marked by an experienced neurologist. The IEDs were epoched around the largest negative peak of the spike with a window of [-330 and 660] ms. The epochs were temporally averaged to obtain a representative multichannel IED waveform per patient. Finally, the average multichannel IED of left temporal lobe epilepsy patients were mirrored so that a consistent right-lateralized EEG topography was obtained. EEG data was organized in a tensor $\mathcal{X}^{EEG} \in \mathbb{R}^{M \times J \times K}$, where $M = 10$ is the number or patients, $J = 21$ is the number of channels and $K = 250$ is the number of samples.

fMRI data were acquired using a 3T MR scanner and analysed in SPM8. Images were realigned, slice-time corrected, normalised to MNI space (voxel size $2 \times 2 \times 2 mm^3$) and spatially smoothed with an isotropic Gaussian kernel of 6 mm full width at half maximum. Subsequently, EEG-correlated fMRI analysis was performed within the general linear model (GLM) framework. The timing of the IEDs convolved with the canonical hemodynamic response function was used as a regressor of interest. The six rigid-body motion correction parameters, the fMRI signal averaged over the lateral ventricles, and the signal averaged over a region within the white matter were included as confounding covariates.

The resulting activations maps (T-maps) of left temporal lobe epilepsy patients were mirrored in order to obtain consistent right-lateralized activation maps. Then, the activation maps were averaged over the patients and thresholded at $|T| > 3$ to obtain a region-of-interest (ROI) mask including clusters which show consistent increase or decrease in BOLD signal during IEDs across patients. The individual unthresholded activation maps were masked using the ROI mask. The resulting images were vectorized and were organized in a matrix $X^{fMRI} \in \mathbb{R}^{M \times L}$, where $M = 10$ is the number of patients and $L = 11923$ is the number of voxels after masking.

III. RESULTS

The multipatient average IED and the GLM-based T-map is shown in Figure 2 (a). The IED is a triphasic wave, starting with a sharp negative peak followed by a positive deflection and finally a slow negative wave. The T-map reveals activations in the right temporal lobe, in accordance with the patients' diagnostics, however, activations are present in the contralateral temporal lobe and the occipital lobe as well. Moreover, deactivations are observed in areas associated with
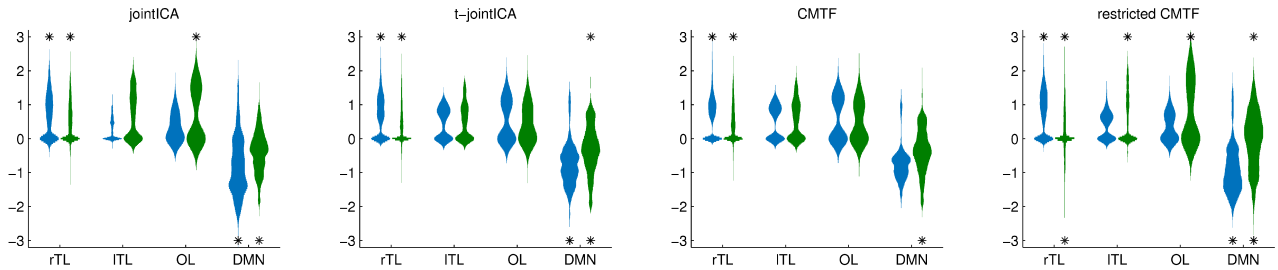
Fig. 3: Voxel intensity distributions in each ROI in each source. The spike and slow wave sources are shown in blue and green, respectively. rTL: right temporal lobe. lTL: left temporal lobe. OL: occipital lobe. DMN: default mode network ECN: executive control network. Asterisks above and below the distributions indicate that a source contains voxels which are significantly activated or deactivated, respectively (at a threshold of $|z| > 2$).

the default mode network (DMN) and beyond. The goal of the joint BSS is to link the diverse temporal EEG features and spatial fMRI features together, hence achieve a better spatio-temporal characterization.

The number of components to extract was chosen as R=2 based on the CPD rank of the EEG part using the core consistency diagnostic. Based on this finding and on medical literature, we hypothesize that the spike and the negative slow wave correspond to 2 different neural processes, i.e. onset and propagation or inhibition. As such, we expect that the true sources are mixed on each patient's EEG and fMRI findings according to the strength of these EEG features. Therefore, we may restrict the solution space by fixing the patient dimension factor matrix A according to the patient-by-patient amplitudes at the peak of the spike and the slow wave. This restriction can be easily implemented in Tensorlab. In what follows, we compare this restricted CMTF approach with unrestricted CMTF, jointICA and t-jointICA. For easy comparison, all signatures were normalized to zero mean and unit standard deviation, i.e. z-scores.

The components extracted with restricted CMTF are visualized in Figure 2 (b) and (c). The first component captures the initial spike part of the EEG, as assessed based on both the temporal signature $\mathbf{p}_1$ and the channel distribution $\mathbf{q}_1$. The corresponding voxel signature shows activation in the right temporal lobe and deactivations in the DMN [1]. The second component captures the slow wave activity: a very pronounced slow wave pattern is observed next to a diminished spike on $\mathbf{p}_2$. The channel signature $\mathbf{q}_2$ also closely resembles the slow wave channel distribution of the average IED. The voxel signature of the second component shows, besides weaker activation in the right temporal lobe, activations in the left temporal lobe and the occipital lobe; and a deactivation pattern resembling the executive control network (ECN).[1]

To compare the results obtained by each of the four approaches, in Figure 3 we visualize the fMRI voxel signatures as voxel intensity distributions within each source and each ROI separately. The EEG time and channel distributions are

[1] based on an atlas containing 90 function ROIs [8] http://findlab.stanford.edu/functional_ROIs.html

very similar to the ones visualized in Figure 2 (b) and (c), therefore, they are not shown again. The distributions in blue correspond to the spike source, while the green distribution correspond to the slow wave source. Each distribution is normalized, so that the bin with the highest count has unit width. Therefore, the shapes of the distributions are comparable. A distribution which is wide at values far from zero indicates a source with significant activations or deactivations. Ideally, the green and blue distributions in a ROI are dissimilar, indicating that activations and deactivations in a ROI are related exclusively either to the spike or to the slow wave. The results are very similar across the methods, leading to the same main observations as explained above. However, jointICA and restricted CMTF distinguish more between the spike and slow wave sources by matching activation in the left temporal lobe and occipital lobe clearly to the latter. Moreover, methods which incorporate multichannel information reveal a clearer deactivation in the DMN related to the spike (distributions shifted towards negative values) and ECN related to the slow wave source. Overall, fixed CMTF achieves the most skewed voxel distributions, therefore, the resulting sources have the most significant activations and deactivations.

Finally, we tested the reproducibility of the source signatures. In other words, we tested how dependent the signatures are on the specific patient data which were included in the analysis. To this end, we rerun the joint BSS algorithms including all possible subsets of 6, 7, 8 or 9 patients. The reproducibility of the sources was quantified by the average pairwise correlation of the fMRI voxel signatures as well as the EEG temporal signatures. The results of this analysis is shown in Figure 4. In general, both the EEG and the fMRI signatures are reasonably reproducible, although EEG signatures are slightly more robust. CMTF provides the most robust fMRI signatures of all approaches, while jointICA and CMTF performs similarly regarding the EEG signatures. As expected, reproducibility decreases with decreasing number of patient data included. From this aspect, the fMRI signatures obtained with restricted CMTF seem to be the most sensitive. Nevertheless, visual inspection confirmed that the main observations regarding the spatiotemporal characteristics of the
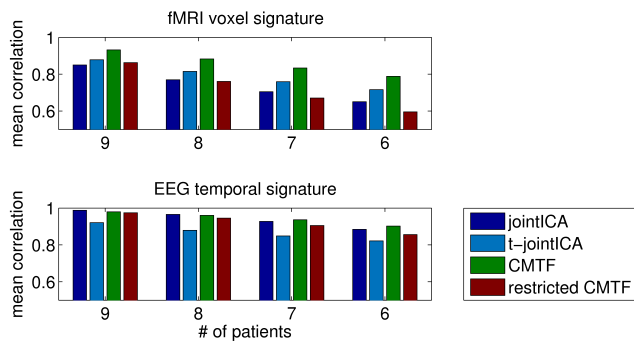
Fig. 4: Reproducibility of the signatures in the different decompositions.

sources still hold.

IV. DISCUSSION

We presented a signal model to fuse group EEG-fMRI data based on the joint factorization of two modalities, where the modalities share a common dimension, i.e. the same variability across patients. This approach relies on some strong assumptions. First, we assumed that all underlying neural sources are reflected on both EEG and fMRI. However, considering that EEG and fMRI measurements work on very different principles and at very different resolutions, one modality can be more sensitive to certain physiological and non-physiological signals than the other and may capture different phenomena. Second, we assumed that both modalities share the same patient-by-patient variability. Nevertheless, it is plausible that the strength of a neural source will not be projected by the same linear function to the EEG and to the fMRI. Therefore, future work will explore more flexible models such as the advanced matrix-tensor decomposition (ACMTF) [9], which allows the presence of both shared and non-shared factors and relaxed ACMTF [10], which allows a similarity rather than equivalence of shared factors. Nevertheless, we believe that careful preprocessing and proper analysis, which are well established in epilepsy imaging, ensured that the input EEG and fMRI data follow closely the assumptions in our CMTF model.

The robustness of the sources against including different subsets of patient data was tested and the reproducibility of the signatures was confirmed. In the future we will try to better understand why jointICA provides stable EEG signatures whereas CMTF clearly extracts more stable fMRI voxel signatures.

We obtained a detailed spatiotemporal characterization of the interictal networks by fusing EEG and fMRI data using joint blind source separation. We extracted two components, corresponding to two distinct neural sources. The signatures of the components show how each neural source is reflected on each modality. To our knowledge, we showed for the first time an association between the different features of the IED (spike and slow wave) and the different regions within the

fMRI activation map found by EEG-correlated fMRI analysis. More specifically, we showed that ipsilateral temporal lobe activation and DMN deactivations are linked to the initial spike phase of the IED, while contralateral temporal and occipital lobe activations as well as ECN deactivations are linked to the later slow wave phase of the IED. Although the interpretation of these findings are out of the scope of this paper, we believe that our approach can lead to new and important insights in epileptic network behaviour.

REFERENCES

[1] D. Lahat, T. Adali, and C. Jutten, "Multimodal data fusion: an overview of methods, challenges, and prospects," *Proceedings of the IEEE*, vol. 103, no. 9, pp. 1449–1477, 2015.

[2] V. Calhoun, T. Adali, G. Pearlson, and K. Kiehl, "Neuronal chronometry of target detection: Fusion of hemodynamic and event–related potential data," *NeuroImage*, vol. 30, no. 2, pp. 544 – 553, 2006.

[3] B. Mijović, K. Vanderperren, N. Novitskiy, B. Vanrumste, P. Stiers, B. Van den Bergh, L. Lagae, S. Sunaert, J. Wagemans, S. Van Huffel *et al.*, "The why and how of jointica: Results from a visual detection task," *NeuroImage*, vol. 60, no. 2, pp. 1171–1185, 2012.

[4] W. Swinnen, B. Hunyadi, E. Acar, S. Van Huffel, and M. De Vos, "Incorporating higher dimensionality in joint decomposition of eeg and fmri," in *Proceedings of the 22nd European Signal Processing Conference (EUSIPCO), Lisbon, 2014 September*. IEEE, 2014, pp. 121–125.

[5] M. Sørensen and L. D. De Lathauwer, "Coupled canonical polyadic decompositions and (coupled) decompositions in multilinear rank-$(l_{r,n}, l_{r,n}, 1)$ terms—part i: Uniqueness," *SIAM Journal on Matrix Analysis and Applications*, vol. 36, no. 2, pp. 496–522, 2015.

[6] L. Sorber, M. Van Barel, and L. De Lathauwer, "Tensorlab v2.0," 2014.

[7] L. Sorber, M. Van Barel, and L. De Lathauwer, "Structured data fusion," *IEEE Journal of Selected Topics in Signal Processing*, vol. 9, no. 4, pp. 586–600, 2015.

[8] W. Shirer, S. Ryali, E. Rykhlevskaia, V. Menon, and M. Greicius, "Decoding subject-driven cognitive states with whole-brain connectivity patterns," *Cerebral cortex*, vol. 22, no. 1, pp. 158–165, 2012.

[9] E. Acar, E. E. Papalexakis, G. Gürdeniz, M. A. Rasmussen, A. J. Lawaetz, M. Nilsson, and R. Bro, "Structure-revealing data fusion," *BMC bioinformatics*, vol. 15, no. 1, pp. 239, 2014.

[10] B. Rivet, M. Duda, A. Guérin-Dugué, C. Jutten, and P. Comon, "Multimodal approach to estimate the ocular movements during eeg recordings: a coupled tensor factorization method," in *37th Annual International Conference of the IEEE Engineering in Medicine and Biology Society (EMBC), Milan, 2015 August*. IEEE, 2015, pp. 6983–6986.

[11] A. Cichocki, D.P. Mandic, A.H. Phan, C.F. Caiafa, G. Zhou, Q. Zhao, and L. De Lathauwer, "Tensor Decompositions for Signal Processing Applications: From two-way to multiway component analysis," *IEEE Signal Processing Magazine*, vol. 32, no. 2., pp. 145–163.